

# Geophysical Research Letters<sup>®</sup>



## RESEARCH LETTER

10.1029/2021GL095266

## Near-Surface Stratification Due to Ice Melt Biases Arctic Air-Sea CO<sub>2</sub> Flux Estimates

### Key Points:

- Seawater CO<sub>2</sub> fugacity ( $f\text{CO}_{2w}$ ) vertical gradients are generated by fresh and cold sea-ice melt water, which lowers surface  $f\text{CO}_{2w}$ .
- Air-sea CO<sub>2</sub> fluxes are biased when estimated using  $f\text{CO}_{2w}$  observations from the sub-surface (6 m depth) in sea-ice melt areas
- Summertime sea-ice melt potentially results in a 6%–17% (with high uncertainty) underestimate of annual Arctic Ocean CO<sub>2</sub> uptake

### Supporting Information:

Supporting Information may be found in the online version of this article.

### Correspondence to:

Y. Dong,  
Yuanxu.Dong@uea.ac.uk

### Citation:

Dong, Y., Yang, M., Bakker, D. C. E., Liss, P. S., Kitidis, V., Brown, I., et al. (2021). Near-surface stratification due to ice melt biases Arctic air-sea CO<sub>2</sub> flux estimates. *Geophysical Research Letters*, 48, e2021GL095266. <https://doi.org/10.1029/2021GL095266>

Received 15 JUL 2021  
Accepted 10 NOV 2021

### Author Contributions:

**Conceptualization:** Yuanxu Dong, Mingxi Yang, Dorothee C. E. Bakker, Peter S. Liss, Thomas G. Bell  
**Data curation:** Yuanxu Dong, Mingxi Yang, Vassilis Kitidis, Ian Brown, Melissa Chierici, Agneta Fransson, Thomas G. Bell  
**Formal analysis:** Yuanxu Dong  
**Funding acquisition:** Mingxi Yang, Thomas G. Bell  
**Investigation:** Mingxi Yang, Vassilis Kitidis, Ian Brown, Melissa Chierici, Agneta Fransson, Thomas G. Bell

© 2021. The Authors.

This is an open access article under the terms of the [Creative Commons Attribution License](https://creativecommons.org/licenses/by/4.0/), which permits use, distribution and reproduction in any medium, provided the original work is properly cited.

Yuanxu Dong<sup>1,2</sup> , Mingxi Yang<sup>2</sup> , Dorothee C. E. Bakker<sup>1</sup> , Peter S. Liss<sup>1</sup>, Vassilis Kitidis<sup>2</sup> , Ian Brown<sup>2</sup>, Melissa Chierici<sup>3,4</sup> , Agneta Fransson<sup>5</sup> , and Thomas G. Bell<sup>2</sup> 

<sup>1</sup>Centre for Ocean and Atmospheric Sciences, School of Environmental Sciences, University of East Anglia, Norwich, UK, <sup>2</sup>Plymouth Marine Laboratory, Plymouth, UK, <sup>3</sup>Fram Centre, Institute of Marine Research, Tromsø, Norway,

<sup>4</sup>Department of Arctic Geophysics, University Centre in Svalbard, Longyearbyen, Norway, <sup>5</sup>Fram Centre, Norwegian Polar Institute, Tromsø, Norway

**Abstract** Air-sea carbon dioxide (CO<sub>2</sub>) flux is generally estimated by the bulk method using upper ocean CO<sub>2</sub> fugacity measurements. In the summertime Arctic, sea-ice melt results in stratification within the upper ocean (top ~10 m), which can bias bulk CO<sub>2</sub> flux estimates when the seawater CO<sub>2</sub> fugacity is taken from a ship's seawater inlet at ~6 m depth ( $f\text{CO}_{2w\_bulk}$ ). Direct flux measurements by eddy covariance are unaffected by near-surface stratification. We use eddy covariance CO<sub>2</sub> flux measurements to infer sea surface CO<sub>2</sub> fugacity ( $f\text{CO}_{2w\_surface}$ ) in the Arctic Ocean. In sea-ice melt regions,  $f\text{CO}_{2w\_surface}$  values are consistently lower than  $f\text{CO}_{2w\_bulk}$  by an average of 39  $\mu\text{atm}$ . Lower  $f\text{CO}_{2w\_surface}$  can be partially accounted for by fresher ( $\geq 27\%$ ) and colder (17%) melt waters. A back-of-the-envelope calculation shows that neglecting the summertime sea-ice melt could lead to a 6%–17% underestimate of the annual Arctic Ocean CO<sub>2</sub> uptake.

**Plain Language Summary** The Arctic Ocean is considered to be a strong sink for atmospheric CO<sub>2</sub>. The air-sea CO<sub>2</sub> flux is almost always estimated indirectly using bulk seawater CO<sub>2</sub> fugacity measured from the ship's seawater inlet at typically ~6 m depth. However, sea-ice melt results in near-surface stratification and can cause a bias in air-sea CO<sub>2</sub> flux estimates if the bulk water CO<sub>2</sub> fugacity is used. The micrometeorological eddy covariance flux technique is not affected by stratification. Here for the first time, we employ eddy covariance measurements to assess the impact of sea-ice melt on Arctic Ocean CO<sub>2</sub> uptake estimates. The results show that the summertime near-surface stratification due to sea-ice melt could lead to an ~10% (with high uncertainty) underestimation of the annual Arctic Ocean CO<sub>2</sub> uptake.

## 1. Introduction

The Arctic Ocean is a strong sink of atmospheric CO<sub>2</sub> due to the active biological production and high CO<sub>2</sub> solubility in cold waters (Anderson et al., 1998; Takahashi et al., 2009). While only accounting for 4% of the world ocean by area and seasonally covered by sea ice, the Arctic Ocean contributes 5%–14% (66–199 Tg C yr<sup>-1</sup>, Bates & Mathis, 2009; Yasunaka et al., 2018) of mean global atmospheric CO<sub>2</sub> removal every year (~1,400 Tg C yr<sup>-1</sup>; Landschützer et al., 2014; Takahashi et al., 2009). However, this Arctic carbon sink is rapidly changing due to climate change. The Arctic warming rate has been more than twice as fast as the global average over the past 5 decades (Romanovsky et al., 2017). The sea-ice extent in the Arctic Ocean in September decreased at a rate of 13.1% decade<sup>-1</sup> during 1979–2020 relative to the 1981–2010 average (Perovich et al., 2020). Sea-ice loss reinforces upper-ocean warming due to reduced surface albedo and increased shortwave penetration, which in turn inhibits sea-ice formation in winter and allows for acceleration of summertime sea-ice loss (Perovich et al., 2007). The reduction in sea-ice coverage in polar regions is expected to increase CO<sub>2</sub> uptake due to larger sea-ice free area, longer sea-ice free period, more freshwater at the surface, and greater biological primary production (Arrigo & van Dijken, 2015; Bates & Mathis, 2009; McPhee et al., 2009; Perovich et al., 2020). However, sea-ice melt also causes near-surface stratification and suppresses water mixing between the surface and sub-surface, which likely generates upper-ocean gradients in temperature, salinity, dissolved inorganic carbon (DIC), total alkalinity (TA) and thus seawater CO<sub>2</sub>.

**Methodology:** Yuanxu Dong, Mingxi Yang, Dorothee C. E. Bakker, Thomas G. Bell

**Project Administration:** Mingxi Yang, Dorothee C. E. Bakker, Thomas G. Bell

**Resources:** Mingxi Yang, Thomas G. Bell

**Software:** Yuanxu Dong

**Supervision:** Mingxi Yang, Dorothee C. E. Bakker, Peter S. Liss, Thomas G. Bell

**Validation:** Yuanxu Dong, Dorothee C. E. Bakker

**Visualization:** Yuanxu Dong

**Writing – original draft:** Yuanxu Dong

**Writing – review & editing:** Yuanxu Dong, Mingxi Yang, Dorothee C. E. Bakker, Peter S. Liss, Vassilis Kitidis, Melissa Chierici, Agneta Fransson, Thomas G. Bell

fugacity (Ahmed et al., 2020; Cai et al., 2010; Calleja et al., 2013; Else et al., 2013; Fransson et al., 2009, 2013; Li et al., 2009; Miller et al., 2019; Rysgaard et al., 2007; Yamamoto-Kawai et al., 2009).

The air-sea CO<sub>2</sub> flux ( $F_{\text{CO}_2}$ , mmol m<sup>-2</sup> day<sup>-1</sup>) is generally estimated indirectly by the bulk equation as the product of the gas transfer velocity and the air-sea gas concentration difference. Accounting for near-surface temperature gradients, Woolf et al. (2016) recommended:

$$F_{\text{CO}_2} = K_{660} \left( \frac{Sc}{660} \right)^{-0.5} (\alpha_{ss} f\text{CO}_{2w} - \alpha_s f\text{CO}_{2a}) \quad (1)$$

where  $K_{660}$  (cm h<sup>-1</sup>) is the gas transfer velocity at a Schmidt number ( $Sc$ ) of 660 (Wanninkhof et al., 2009).  $K_{660}$  is usually parameterized as a function of wind speed (e.g., Nightingale et al., 2000).  $\alpha_{ss}$  and  $\alpha_s$  are the CO<sub>2</sub> solubility (mol L<sup>-1</sup> atm<sup>-1</sup>, Weiss, 1974) in the subskin and skin seawater, respectively (Woolf et al., 2016).  $f\text{CO}_{2w}$  and  $f\text{CO}_{2a}$  are the CO<sub>2</sub> fugacity ( $\mu\text{atm}$ ) near the sea surface and in the overlying atmosphere, respectively. Similarly, the air-sea sensible heat flux can be estimated by the bulk method using a parameterized sensible heat transfer velocity and the sea-air temperature difference (Text S1 in Supporting Information S1).

Air-sea exchange of sparingly soluble gases (e.g., CO<sub>2</sub>) is limited mostly by transport within the waterside molecular diffusive layer (MDL, 20–200  $\mu\text{m}$  depth; Jähne, 2009) just beneath the water surface (Liss & Slater, 1974). Thus,  $f\text{CO}_{2w}$  represents the CO<sub>2</sub> fugacity at the base of MDL ( $f\text{CO}_{2w\_surface}$ ). In practice,  $f\text{CO}_{2w}$  measurements are generally made on bulk seawater from the ship's underway inlet (~6 m depth,  $f\text{CO}_{2w\_bulk}$ ). For convenience, the upper several meters of the ocean are assumed to be homogeneous in bulk flux calculations (i.e.,  $f\text{CO}_{2w} = f\text{CO}_{2w\_surface} = f\text{CO}_{2w\_bulk}$ ).

However, incidences of near-surface stratification call into question the vertical homogeneity assumption. In the Arctic, three sea-ice-related mechanisms likely drive near-surface vertical gradients in CO<sub>2</sub>: (a) Brine drainage. When sea ice forms, carbonate species, and salt are ejected into the water under the sea ice as part of brine drainage (e.g., Fransson et al., 2013), which depletes the CO<sub>2</sub> within the sea ice. The salty, dense water sinks and is eventually sequestered in the deep ocean (Rudels et al., 2005). (b) Surface photosynthesis. Phytoplankton are often found in the bottom ice or beneath the Arctic sea ice and their photosynthetic activity further reduces the CO<sub>2</sub> concentration within the sea ice (Assmy et al., 2017; Fransson et al., 2013, 2017). (c) Ikaite dissolution. Dissolution of sea-ice derived ikaite will consume CO<sub>2</sub> in Arctic surface waters (Chierici et al., 2019; Fransson et al., 2017). The latest measurements in the Arctic coastal waters show significant vertical  $f\text{CO}_{2w}$  gradients in the upper ocean (Ahmed et al., 2020; Miller et al., 2019). Miller et al. (2019) show both positive and negative  $f\text{CO}_{2w}$  gradients without separating the contributions of sea-ice melt and river runoff. Ahmed et al. (2020) show consistently negative gradients (i.e.,  $f\text{CO}_{2w\_surface} < f\text{CO}_{2w\_bulk}$ ) in the sea-ice melt regions. Vertical gradients, if left unaccounted for, will result in a bias in bulk air-sea CO<sub>2</sub> flux estimates.

The micrometeorological eddy covariance (EC) method derives CO<sub>2</sub> fluxes directly and represents an alternative approach for understanding Arctic air-sea CO<sub>2</sub> exchange. EC does not rely on seawater measurements (Text S2 in Supporting Information S1), and thus EC fluxes are not affected by near-surface vertical variation in seawater properties. However, polar oceans are a hostile environment and reliable direct CO<sub>2</sub> flux measurements by EC are scarce (Butterworth & Else, 2018; Butterworth & Miller, 2016; Prytherch & Yelland, 2021; Prytherch et al., 2017). This paper presents EC CO<sub>2</sub> and sensible heat flux data from two Changing Arctic Ocean Program cruises. Directly measured fluxes were used to compute the implied sea surface  $f\text{CO}_{2w}$  and water temperature ( $f\text{CO}_{2w\_surface}$ ,  $T_{w\_surface}$ ). Comparisons of implied surface values with bulk measurements enable us to assess the impact of vertical gradients on bulk air-sea CO<sub>2</sub> flux estimates. We further speculate on the influence of near-surface stratification on bulk air-sea CO<sub>2</sub> flux estimates for the entire Arctic Ocean.

## 2. Methods

### 2.1. Description of Cruises

Cruise tracks of JR18006 and JR18007 (on RRS *James Clark Ross*, JCR) and FS2019 (on RV *Kronprins Haakon*) are shown in Figure S1 in Supporting Information S1. JR18006 visited the Barents Sea between

June 28 and August 1 2019. JR18007 targeted the Fram Strait region within the Greenland Sea between August 4 and 30 2019. DIC and TA were not measured during JR18006 and JR18007. Measurements taken between September 2 and 5, 2019 (between 0° and 10°W) on cruise FS2019 were used to constrain the upper ocean carbonate system. Methods for DIC and TA measurements can be found in Chierici et al. (2019). The EC system on JCR, processing and quality control of fluxes, underway measurements, and the meteorological observations are detailed elsewhere (Dong et al., 2021) and are briefly described in Text S3 in Supporting Information S1.  $fCO_{2w}$  measurements were only available during ice-free periods of JR18007.

## 2.2. Implied Surface Variables From Eddy Covariance Fluxes

We use Brunt-Väisälä frequency ( $N^2$ ) threshold to identify stratified waters.  $N^2$  at ~6 m depth is calculated from the CTD (conductivity, temperature, depth) profiles ( $N^2 = -g(\rho_{7m} - \rho_{5m}) / (2 * \rho_{7m})$ ) with gravitational acceleration  $g$  and seawater density  $\rho$ ). Fischer et al. (2019) used  $N^2 \geq 10^{-4} s^{-2}$  in upwelling waters, but we expect the threshold for near-surface stratification to be more evident in regions with sea-ice melt, so use a more robust threshold of  $N^2 \geq 10^{-3} s^{-2}$ . Measurements in waters without a CTD cast and salinity below 34.5 are marked as having an ‘unknown’ stratification status.

The derivations of EC air-sea  $CO_2$  flux ( $F_{CO_2-EC}$ ) and sensible heat flux ( $H_{S-EC}$ ) are detailed in Text S2 in Supporting Information S1. The gas transfer velocity (hourly) is computed by replacing the bulk flux with the hourly EC flux in a rearrangement of Equation 1:

$$K_{660} = \frac{F_{CO_2-EC}}{(Sc / 660)^{-0.5} (\alpha_{ss} fCO_{2w\_bulk} - \alpha_s fCO_{2a})} \quad (2)$$

In regions with near-surface stratification,  $fCO_{2w\_bulk}$  may not be representative of the surface (i.e.,  $fCO_{2w\_bulk} \neq fCO_{2w\_surface}$ ). Therefore, to derive a wind speed ( $U_{10N}$ ) dependent parametrization of  $K_{660}$  from this project ( $K_{660\_u}$ ), only data from non-stratified waters are considered.  $K_{660\_u}$  and the EC  $CO_2$  flux observations are then used to compute the implied  $fCO_{2w\_surface}$  for all water types (non-stratified and stratified):

$$fCO_{2w\_surface} = \frac{F_{CO_2-EC}}{K_{660\_u} (Sc / 660)^{-0.5} \alpha_{ss}} + \frac{\alpha_s}{\alpha_{ss}} fCO_{2a} \quad (3)$$

A similar approach is used to derive sensible heat transfer velocity ( $K_H$ ) and compute the implied surface seawater temperature ( $T_{w\_surface}$ ):

$$K_H = \frac{H_{S-EC}}{\rho_a c_{pa} (T_{w\_bulk} - dT - T_a)} \quad (4)$$

$$T_{w\_surface} = \frac{H_{S-EC}}{\rho_a c_{pa} K_{H\_u}} + T_a \quad (5)$$

where  $K_H$  ( $cm\ h^{-1}$ ) is parametrized with  $U_{10N}$  ( $K_{H\_u}$ ) using data from non-stratified waters (Figure S2 in Supporting Information S1). Here,  $\rho_a$  ( $kg\ m^{-3}$ ) is the mean density of dry air,  $c_{pa}$  ( $J\ kg^{-1}\ K^{-1}$ ) is the heat capacity of air and  $T_a$  (K) is the air temperature. The temperature offset due to the cool skin effect,  $dT$  (K), is estimated using the COARE 3.5 model (Edson et al., 2013; Fairall et al., 1996).

## 3. Results and Discussion

### 3.1. $CO_2$ Flux Time Series

The time series of hourly averaged EC and bulk fluxes for  $CO_2$  and heat are shown for cruise JR18007 (Figure 1). The bulk  $CO_2$  flux is calculated from  $fCO_{2w\_bulk}$ ,  $fCO_{2a}$ , and  $T_{w\_bulk}$  measurements using the gas transfer velocity parametrization from Nightingale et al. (2000). The bulk sensible heat flux is computed using the COARE 3.5 model (Edson et al., 2013). The sea ice concentration (Figure 1d) is derived from the Advanced Microwave Scanning Radiometer-Earth Observing System (AMSR-E, daily and 3.125 km resolution; Spreen et al., 2008).

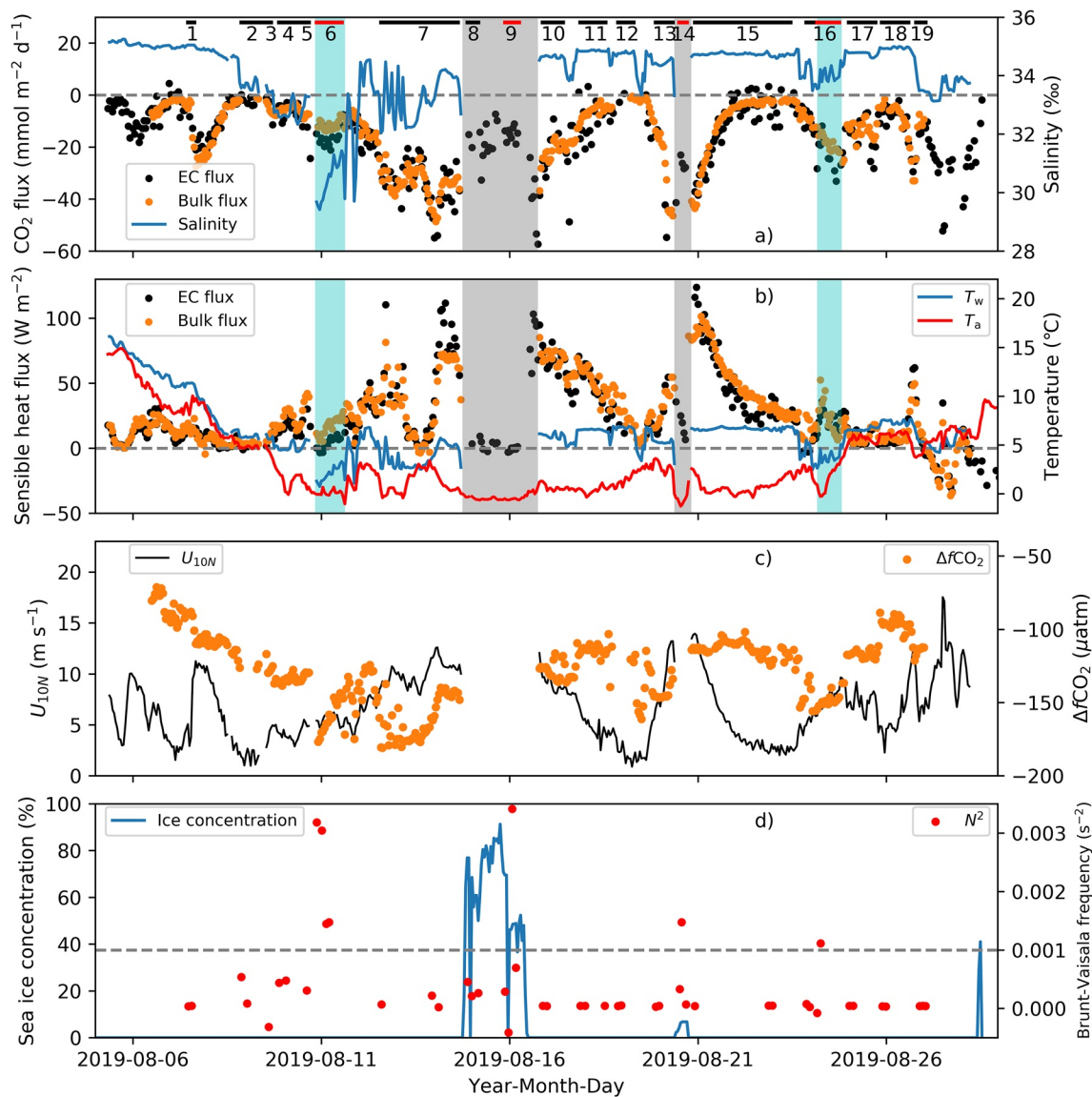


**Figure 1.** Time series of hourly fluxes and environmental variables on JR18007. Negative (positive) fluxes represent ocean sinks (sources): (a) EC and bulk air-sea  $\text{CO}_2$  fluxes, and salinity at 6 m depth. Light blue shading shows near-surface stratification (identified from conductivity, temperature, depth [CTD] profiles). Gray shading indicates ice-covered waters where the underway seawater system was shut off. Dashes on the top axis correspond to CTD stations. Stations with near-surface stratification are in red. Dash length represents the duration on station; (b) EC and bulk sensible heat flux, seawater temperature ( $T_w$ ) at 6 m depth and air temperature ( $T_a$ ); (c) 10-m neutral wind speed and air-sea  $\text{CO}_2$  fugacity difference ( $\Delta f\text{CO}_2 = f\text{CO}_{2w\_bulk} - f\text{CO}_{2a}$ ); (d) Sea ice concentration (Spren et al., 2008) and Brunt-Väisälä frequency ( $N^2$ ) at 6 m depth.

Stratified areas were located at the edge of or within the sea ice (Figure S1 in Supporting Information S1), with relatively low near-surface salinity and temperature (Figure 1) suggesting that sea-ice melt is the principal reason for near-surface stratification. Terrestrial runoff as a source of freshwater is unlikely because the ship was far from land (>50 km) in the stratified stations (Figure S1 in Supporting Information S1). Furthermore, there were no significant precipitation events during the cruise, ruling out surface freshening due to precipitation.

The relatively good agreement between EC fluxes and bulk air-sea  $\text{CO}_2$  fluxes in non-stratified regions (Figure 1a and Figure S3 in Supporting Information S1) suggests that the data (EC fluxes and underway  $f\text{CO}_{2w\_bulk}$ ) are reliable and that the Nightingale et al. (2000) gas transfer velocity parameterization is reasonable for this study region. In areas with near-surface stratification (stations 6 and 16), bulk  $\text{CO}_2$  fluxes

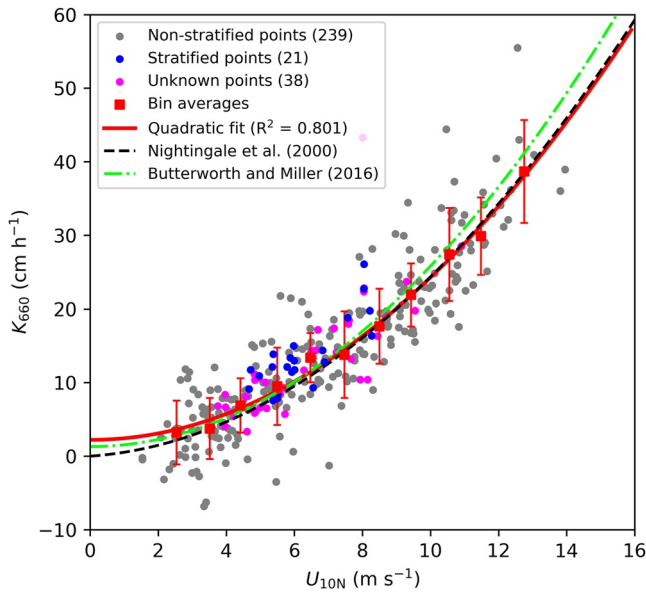


**Figure 2.** Relationship between the  $\text{CO}_2$  gas transfer velocity ( $K_{660}$ , derived from hourly eddy covariance air-sea  $\text{CO}_2$  flux measurements) and wind speed ( $U_{10N}$ ) during JR18007. Gray dots represent  $K_{660}$  in non-stratified waters, blue dots correspond to  $K_{660}$  in stratified waters, and magenta dots indicate data with unknown stratification status. Red squares are  $1 \text{ m s}^{-1}$  bin averages of the non-stratified values, with error bars representing 1 standard deviation. The red curve is a quadratic parameterization ( $K_{660,u} = 0.220 U_{10N}^2 + 2.213$ ;  $R^2 = 0.801$ ). The  $K_{660}$  parameterizations of Nightingale et al. (2000) (black dashed) and Butterworth and Miller (2016) (green dot dashed) are also shown.

fit. The fit ( $K_{660,u} = 0.220 U_{10N}^2 + 2.213$ ) agrees fairly well with a widely-used  $K_{660}$  parameterization based on dual tracer results (Nightingale et al., 2000) and a more recent parameterization derived from EC air-sea  $\text{CO}_2$  flux measurements (Butterworth & Miller, 2016).

The  $K_{660}$  data in stratified waters (21 hourly  $K_{660}$ ) are consistently higher than the parameterized  $K_{660,u}$  curve. Including data from stratified waters and waters with unknown stratification status (38 hourly  $K_{660}$ ) decreases the strength of the quadratic fit between hourly  $K_{660}$  and  $U_{10N}$  from  $R^2 = 0.801$  to  $R^2 = 0.777$  (Table S1 in Supporting Information S1). This is most likely due to a vertical gradient in  $f\text{CO}_{2w}$ , where  $f\text{CO}_{2w,\text{bulk}}$  systematically exceeds  $f\text{CO}_{2w,\text{surface}}$  (see Section 3.3).

### 3.3. Implied Sea Surface $\text{CO}_2$ Fugacity and Temperature

The  $K_{660}$  parameterization in Figure 2 and the  $K_H$  parameterizations (Figure S2 in Supporting Information S1) are used for estimating  $f\text{CO}_{2w,\text{surface}}$  (Equation 3) and  $T_{w,\text{surface}}$  (Equation 5). Data at low wind speeds ( $U_{10N} < 4 \text{ m s}^{-1}$ ) are excluded from these calculations because of the low signal-to-noise ratios of EC fluxes and larger relative uncertainties in transfer velocities during calm conditions (Dong et al., 2021).

Figure 3 shows the comparison between hourly averages of the bulk seawater measurements ( $f\text{CO}_{2w,\text{bulk}}$  and, in the case of temperature, adjusted for the cool skin:  $T_w - dT$ ) and the implied surface values ( $f\text{CO}_{2w,\text{surface}}$  and  $T_{w,\text{surface}}$ ). In non-stratified waters (gray dots in Figure 3a), the means of the two  $f\text{CO}_{2w}$  values compare reasonably well, even though the  $f\text{CO}_{2w,\text{surface}}$  values have a larger range than  $f\text{CO}_{2w,\text{bulk}}$  due to variability in the EC  $\text{CO}_2$  flux observations and the uncertainty in the  $K_{660}$  parameterization. In stratified waters (blue dots in Figure 3a), the implied  $f\text{CO}_{2w,\text{surface}}$  values are consistently lower than  $f\text{CO}_{2w,\text{bulk}}$ , indicating that bulk measurements are not representative of the surface. Similarly, EC implied  $T_{w,\text{surface}}$  values are consistently lower than the bulk water temperature in low salinity areas ( $\leq 32$ , Figure 3b). These data corroborate the

are consistently less negative (lower in magnitude) than EC  $\text{CO}_2$  fluxes (Figure 1a). Meanwhile, bulk sensible heat fluxes are slightly higher than EC fluxes in stratified regions.

Another intriguing feature is that EC sensible heat fluxes were close to zero during sea ice stations 8 and 9, but EC  $\text{CO}_2$  fluxes were still significant. The sea ice concentration data (Figure 1d) show that the sea surface was not fully ice-covered in this region. One possible reason for near-zero sensible heat flux but detectable  $\text{CO}_2$  flux is that the surface (seawater or sea ice) temperature was close to the air temperature, while an  $f\text{CO}_2$  gradient existed across the sea surface. Also, air-sea  $\text{CO}_2$  exchange is mainly controlled by waterside processes (Liss & Slater, 1974), whereas the air-sea heat exchange is controlled by airside processes (Yang et al., 2016). The impact of sea ice on waterside controlled gases (e.g.,  $\text{CO}_2$ ) may be different from the impact on airside controlled gases and heat.

### 3.2. Gas Transfer Velocity

Dong et al. (2021) show that the hourly EC air-sea  $\text{CO}_2$  flux relative uncertainty is  $\sim 20\%$  on average during JR18007. The  $\Delta f\text{CO}_2$  ( $= f\text{CO}_{2w,\text{bulk}} - f\text{CO}_{2a}$ ) ranges from  $-181$  to  $-71 \mu\text{atm}$  ( $-130 \mu\text{atm}$  on average, Figure 1c) during JR18007. The relatively low flux uncertainty and large  $\Delta f\text{CO}_2$  values enable us to estimate the gas transfer velocity ( $K_{660}$ ) with high accuracy. Figure 2 shows  $K_{660}$  derived from quality-controlled EC  $\text{CO}_2$  fluxes and  $\Delta f\text{CO}_2$  observations, plotted against 10-m neutral wind speed ( $U_{10N}$ ); the latter is determined from measurements of wind speed adjusted to  $U_{10N}$  using the COARE 3.5 model (Edson et al., 2013). There are 298 hourly averaged  $K_{660}$  values. 239 hourly  $K_{660}$  values from non-stratified waters are binned in wind speed intervals of  $1 \text{ m s}^{-1}$  and the bin averages (red squares) are used to derive a least square quadratic

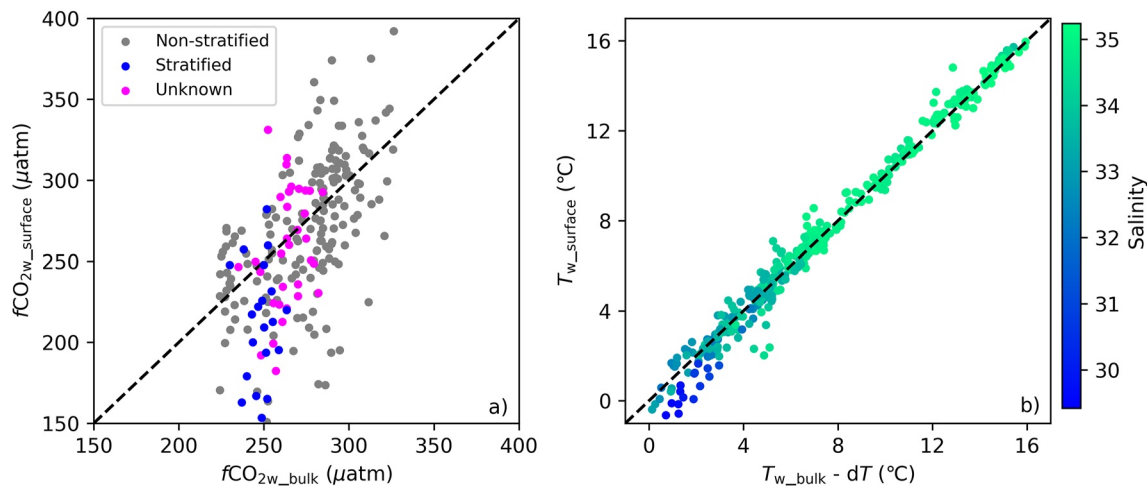


**Figure 3.** Measurements at 6 m depth of seawater  $\text{CO}_2$  fugacity ( $f\text{CO}_{2w\_bulk}$ ) and temperature (corrected for the cool skin effect, that is,  $T_{w\_bulk} - dT$ ) versus eddy covariance implied sea surface  $\text{CO}_2$  fugacity ( $f\text{CO}_{2w\_surface}$ ) and temperature ( $T_{w\_surface}$ ): (a)  $f\text{CO}_2$  values from cruise JR18007. Gray dots are values in non-stratified waters, blue dots are in stratified waters and magenta dots are in waters for which the stratification status could not be determined; (b) Seawater temperature for JR18006 and JR18007 with the dots color-coded by salinity at 6 m depth.

CTD profiles from JR18007 (Figure S4 in Supporting Information S1) and suggest that the surface water is colder and fresher than bulk water in regions with sea-ice melt.

Within the stratified areas during JR18007,  $f\text{CO}_{2w\_surface}$  (mean =  $208 \mu\text{atm}$ ) is on average  $39 \pm 39 \mu\text{atm}$  lower than  $f\text{CO}_{2w\_bulk}$  (mean =  $247 \mu\text{atm}$ ), while  $T_{w\_surface}$  is on average  $0.7 \pm 0.8 \text{ }^\circ\text{C}$  below  $T_{w\_bulk} - dT$ . A temperature change of  $0.7 \text{ }^\circ\text{C}$  should reduce  $f\text{CO}_{2w}$  by  $7 \mu\text{atm}$  according to the Takahashi et al. (1993) empirical temperature relationship (Equation S5 in Supporting Information S1), suggesting that the temperature effect accounts for 18% of the vertical  $f\text{CO}_{2w}$  gradient within the stratified area.

Although the top 4 m depth CTD data have been removed due to ship interferences and rough sea state, CTD profiles still indicate that seawater at 4 m depth is fresher than the 5–10 m water at the stratified stations (Figure S4 in Supporting Information S1). The shapes of near-surface salinity profiles generally mirror those of temperature profiles (i.e., the vertical salinity gradient is nearly the same as the temperature gradient in magnitude; Figure S4 in Supporting Information S1). Here we crudely assume that the salinity difference between the sea surface and 6 m depth is 0.7 (i.e., corresponding to the temperature difference of  $0.7^\circ\text{C}$ ). Variations in near-surface salinity alter carbonate chemistry and influence  $f\text{CO}_{2w}$ . We use bulk water ( $\sim 6$  m depth) DIC and TA measurements (Table S2 in Supporting Information S1) collected a month later from nine stations in the nearby Fram Strait (Figure S1 in Supporting Information S1, the sea ice concentration had decreased from  $\sim 50\%$  to  $\sim 0\%$  during a previous week of the cruise) to estimate the influence of salinity change on the vertical  $f\text{CO}_{2w}$  gradient. The average DIC, TA, and salinity were  $1,974 \pm 19 \mu\text{mol kg}^{-1}$ ,  $2,100 \pm 22 \mu\text{mol kg}^{-1}$ , and  $30.6 \pm 0.6$ , respectively.

Bulk water DIC and TA are corrected to a sea surface salinity by dividing by bulk salinity and multiplying by surface salinity (= bulk salinity  $- 0.7$ ). The calculated surface and measured bulk water DIC and TA are used to estimate the sensitivity in  $f\text{CO}_{2w}$  to salinity change (Lewis & Wallace, 1998; Van Heuven et al., 2011). We estimate that the vertical salinity gradient can explain a  $f\text{CO}_{2w}$  gradient of on average  $10.6 \pm 1.1 \mu\text{atm}$ . This salinity-related decrease in  $f\text{CO}_{2w}$  accounts for 27% of the near-surface vertical  $f\text{CO}_{2w}$  gradient. Considering that the surface seawater is expected to be rapidly warmed by solar radiation, whereas salinity is less affected by surface warming, the temperature effect will be more transitory than the salinity effect. Thus, the estimated salinity effect is likely conservative, that is, greater than 27%.

Sea-ice-related plankton metabolism might be another reason for lower  $f\text{CO}_{2w}$  in the surface stratified layer. The CTD oxygen profiles show that the oxygen concentration increases close to the surface in the stratified stations (Figure S4 in Supporting Information S1). Chierici et al. (2019) observed meltwater-induced

phytoplankton production in the marginal ice zone near Fram Strait in May 2019, which continued until the end of August. Photosynthesis in the upper few meters of the water column could reduce  $f\text{CO}_{2w}$ .

Air-sea gas exchange cannot be the cause of the lower surface  $f\text{CO}_{2w}$  observed in stratified waters because the influx of  $\text{CO}_2$  would have not helped to explain the observations, increasing  $f\text{CO}_{2w}$  at the surface. The results presented here demonstrate that near-surface stratification due to sea-ice melt generates a strong near-surface  $f\text{CO}_{2w}$  gradient ( $f\text{CO}_{2w,\text{surface}} < f\text{CO}_{2w,\text{bulk}}$ ), which causes a bias in bulk air-sea  $\text{CO}_2$  flux estimates when  $f\text{CO}_{2w,\text{bulk}}$  from  $\sim 6$  m depth is used. In the next section, we estimate the impact such a bias would have on  $\text{CO}_2$  uptake by the entire Arctic Ocean.

### 3.4. Potential Impact on Arctic Ocean $\text{CO}_2$ Uptake Estimates

Here we speculate on the potential impact of near-surface stratification due to summertime sea-ice melt on estimates of  $\text{CO}_2$  uptake for the entire Arctic Ocean.

We make the following crude assumptions: (a) bulk  $f\text{CO}_{2w}$  measurements overestimate the surface  $f\text{CO}_{2w}$  in all regions with sea-ice melt; (b) the  $f\text{CO}_{2w}$  overestimation ( $-f\text{CO}_{2w}$  offset,  $\mu\text{atm}$ ) decreases with wind speed for  $U_{10N} > 3 \text{ m s}^{-1}$  ( $f\text{CO}_{2w}$  offset =  $-408 U_{10N}^{-1} + 27$ , Figure S5 in Supporting Information S1) (Ahmed et al., 2020; Fischer et al., 2019; Miller et al., 2019) and is assumed to be constant ( $109 \mu\text{atm}$ ) at  $U_{10N} \leq 3 \text{ m s}^{-1}$ ; (c) surface seawater temperature and salinity are  $2^\circ\text{C}$  and 31 within the stratified areas, respectively (average of the EC implied  $T_{w,\text{surface}}$  and surface salinity in the stratified waters during JR18007).

The 6-hr Cross-Calibrated Multi-Platform (CCMP) Wind Vector Analysis (Atlas et al., 2011) at a height of 10 m above mean sea level is used to calculate  $K_{660}$  and to estimate the  $f\text{CO}_{2w}$  offset. The flux offset is calculated with Equation 1 (replacing  $\Delta f\text{CO}_2$  with  $f\text{CO}_{2w}$  offset), and the result from each grid cell is linearly scaled using the sea ice concentration. The AMSR-E (Spreen et al., 2008) daily sea ice concentration (SIC) data (3.125 km grid resolution) are used to determine the extent of stratified areas. There are two scenarios when a grid cell is deemed to contain near-surface stratified water: (a) the ice-free proportion of the grid cell is considered to be stratified when SIC is between 0% and 100%; (b) SIC of a grid cell has declined to 0% during the last 10 days (assuming that near-surface stratification lasts for 10 days, within the indicated duration time indicated by Ahmed et al., 2020), the whole cell is considered to be stratified.

We focus on the summertime (June to August inclusive) the Arctic Ocean in 2019. The result shows that the largest area with near-surface stratification and the greatest underestimation of  $\text{CO}_2$  uptake occur in July (Figure S6 in Supporting Information S1).  $K_{660}$  increases with the wind speed, while the magnitude of  $f\text{CO}_{2w}$  offset decreases with wind speed, so the wind speed effect on the variability of the flux offset is almost canceled out and the estimated bulk flux variability is mainly related to the size of the stratified area. The integrated summertime underestimation of Arctic Ocean  $\text{CO}_2$  uptake due to sea-ice melt is estimated to be 11 Tg C, which is comparable with the back-of-the-envelope calculation ( $9.3 \text{ Tg C yr}^{-1}$ ) of Ahmed et al. (2020).

The above estimate is based on assumptions that the  $f\text{CO}_{2w}$  offset is wind speed dependent and the shallow stratification lasts for 10 days. High wind speed enhances the near-surface seawater mixing and weakens the shallow stratification. We do not have a robust relationship between  $f\text{CO}_{2w}$  offset and wind speed because our measurements in stratified waters only span a small range of wind speeds ( $6 \pm 1 \text{ m s}^{-1}$ ) and the data are quite scattered (Figure S5 in Supporting Information S1). If we do not consider the influence of wind speed on the  $f\text{CO}_{2w}$  gradient and assume a constant  $f\text{CO}_{2w}$  offset of  $-39 \mu\text{atm}$  in the sea ice melt region, then the underestimation of Arctic Ocean  $\text{CO}_2$  uptake is reduced to 6 Tg C. Another major uncertainty is inherent in our assumption that near-surface stratification lasts for 10 days. If we assume that the near-surface stratification lasts 7 days or 14 days, the underestimation of Arctic Ocean  $\text{CO}_2$  uptake is 10 Tg C and 13 Tg C, respectively (using the wind speed dependent  $f\text{CO}_{2w}$  offset).

The underestimation of 11 Tg C in 2019 corresponds to 6%–17% of annual Arctic Ocean carbon uptake ( $66\text{--}199 \text{ Tg C yr}^{-1}$ , Bates & Mathis, 2009). Note that the  $\text{CO}_2$  sink estimate by Bates and Mathis (2009) was a decade ago, so the percentage of this underestimate may have slightly changed.

#### 4. Conclusions

This study reports direct and indirect estimates of air-sea CO<sub>2</sub> and sensible heat fluxes from shipboard campaigns in the summertime Arctic Ocean. Direct fluxes by eddy covariance are used to compute the implied sea surface  $f\text{CO}_{2w}$  and  $T_w$ . Comparisons of implied surface values with bulk water measurements at 6 m depth help to identify possible vertical  $f\text{CO}_{2w}$  gradients in the upper ocean. Implied surface  $f\text{CO}_{2w}$  is on average 39  $\mu\text{atm}$  lower than bulk  $f\text{CO}_{2w}$  in regions with near-surface stratification due to sea ice melt. EC-derived gas transfer velocities ( $K_{660}$ ) using bulk seawater measurements in non-stratified regions agree well with previous parameterizations. However, in stratified regions, EC-derived  $K_{660}$  is higher at a given wind speed because of the near-surface  $f\text{CO}_{2w}$  gradient.

Cooling and freshening due to sea-ice melt in the Arctic summer account for 18% and at least 27% of the near-surface  $f\text{CO}_{2w}$  gradient during cruise JR18007, respectively. Enhanced photosynthesis in the stratified layer may also have contributed to the near-surface  $f\text{CO}_{2w}$  gradient.

The Arctic Ocean is an important CO<sub>2</sub> sink, but this ocean carbon uptake may have been underestimated previously due to near-surface  $f\text{CO}_{2w}$  gradients induced by sea-ice melt. A simple calculation for the summertime Arctic Ocean suggests that near-surface stratification due to sea-ice melt could lead to an  $\sim 10$  Tg C underestimation of CO<sub>2</sub> uptake but there is considerable uncertainty in the validity of such an extrapolation. The continuing loss of Arctic sea ice is expected to increase CO<sub>2</sub> uptake in summer, and may further increase the uncertainty in Arctic air-sea CO<sub>2</sub> flux estimates if near-surface stratification is not considered.

This is the first time to our knowledge that direct measurements by EC have been used to quantify the potential bias in bulk flux estimates due to near-surface stratification in the Arctic Ocean. A similar underestimation in CO<sub>2</sub> flux related to sea-ice melt may also occur in the Southern Ocean. Detailed studies of upper ocean (0–10 m) gradients in  $f\text{CO}_{2w}$ , temperature, salinity, DIC, TA, and biological rates along with EC flux measurements, are required to improve understanding of sea-ice melt impacts and near-surface stratification on air-sea exchange.

#### Data Availability Statement

The raw EC data and hourly flux data can be accessed at: <https://doi.org/10.5285/03C78C45-08B5-4D82-B09D-09C0B8A32C4D>. The CTD profile data are stored at the British Oceanographic Data Center (BODC): [https://www.bodc.ac.uk/data/bodc\\_database/nodb/cruise/17335/](https://www.bodc.ac.uk/data/bodc_database/nodb/cruise/17335/). AMSR-E data: [https://seaice.uni-bremen.de/data/amr2/asi\\_daygrid\\_swath/n3125/](https://seaice.uni-bremen.de/data/amr2/asi_daygrid_swath/n3125/). CCMP data: <http://data.remss.com/ccmp/v02.1.NRT/>.

#### Acknowledgments

The Natural Environment Research Council (NERC) supported the Arctic research campaigns (DIAPOD, NE/P006280/2; ChAOS, NE/P006493/1 and PETRA, NE/R012830/1). CO<sub>2</sub> flux measurements were made possible by funding from the NERC ORCHESTRA (NE/N018095/1) and European Space Agency AMT4oceanSatFluxCCN (4000125730/18/NL/FF/gp) projects. DIC/TA data were supported by the Flagship program “Ocean Acidification and effects in northern waters” within the FRAM-High North Research Centre for Climate and Environment, Tromsø, Norway. The authors thank captains and crew of RRS *James Clark Ross* and all those who helped keep the CO<sub>2</sub> flux system running. The authors thank Robyn Owen (BODC) for her kind help with the CTD profile data. The analysis of these data is supported by the China Scholarship Council (CSC/201906330072).

#### References

- Ahmed, M. M. M., Else, B. G. T., Capelle, D., Miller, L. A., & Papakyriakou, T. (2020). Underestimation of surface  $p\text{CO}_2$  and air-sea CO<sub>2</sub> fluxes due to freshwater stratification in an Arctic shelf sea, Hudson Bay. *Elementa: Science of the Anthropocene*, 8(1), 084. <https://doi.org/10.1525/elementa.084>
- Anderson, L. G., Olsson, K., & Chierici, M. (1998). A carbon budget for the Arctic Ocean. *Global Biogeochemical Cycles*, 12(3), 455–465. <https://doi.org/10.1029/98GB01372>
- Arrigo, K. R., & van Dijken, G. L. (2015). Continued increases in Arctic Ocean primary production. *Progress in Oceanography*, 136, 60–70. <https://doi.org/10.1016/j.pocean.2015.05.002>
- Assmy, P., Fernández-Méndez, M., Duarte, P., Meyer, A., Randelhoff, A., Mundy, C. J., et al. (2017). Leads in Arctic pack ice enable early phytoplankton blooms below snow-covered sea ice. *Scientific Reports*, 7 (40850), 1–9. <https://doi.org/10.1038/srep40850>
- Atlas, R., Hoffman, R. N., Ardizzone, J., Leidner, S. M., Jusem, J. C., Smith, D. K., & Gombos, D. (2011). A cross-calibrated, multiplatform ocean surface wind velocity product for meteorological and oceanographic applications. *Bulletin of the American Meteorological Society*, 92(2), 157–174. <https://doi.org/10.1175/2010BAMS2946.1>
- Bates, N. R., & Mathis, J. T. (2009). The Arctic Ocean marine carbon cycle: Evaluation of air-sea CO<sub>2</sub> exchanges, ocean acidification impacts and potential feedbacks. *Biogeosciences*, 6(11). <https://doi.org/10.5194/bg-6-2433-2009>
- Butterworth, B. J., & Else, B. G. T. (2018). Dried, closed-path eddy covariance method for measuring carbon dioxide flux over sea ice. *Atmospheric Measurement Techniques*, 11(11), 6075–6090. <https://doi.org/10.5194/amt-11-6075-2018>
- Butterworth, B. J., & Miller, S. D. (2016). Air-sea exchange of carbon dioxide in the Southern Ocean and Antarctic marginal ice zone. *Geophysical Research Letters*, 43(13), 7223–7230. <https://doi.org/10.1002/2016GL069581>
- Cai, W.-J., Chen, L., Chen, B., Gao, Z., Lee, S. H., Chen, J., et al. (2010). Decrease in the CO<sub>2</sub> uptake capacity in an ice-free Arctic Ocean basin. *Science*, 329(5991), 556–559. <https://doi.org/10.1126/science.1189338>
- Calleja, M. L., Duarte, C. M., Álvarez, M., Vaquer-Sunyer, R., Agustí, S., & Herndl, G. J. (2013). Prevalence of strong vertical CO<sub>2</sub> and O<sub>2</sub> variability in the top meters of the ocean. *Global Biogeochemical Cycles*, 27(3), 941–949. <https://doi.org/10.1002/gbc.20081>
- Chierici, M., Vernet, M., Fransson, A., & Børsheim, K. Y. (2019). Net community production and carbon exchange from winter to summer in the Atlantic water inflow to the Arctic Ocean. *Frontiers in Marine Science*, 6, 1–24. <https://doi.org/10.3389/fmars.2019.00528>

- Dong, Y., Yang, M., Bakker, D. C. E., Kitidis, V., & Bell, T. G. (2021). Uncertainties in eddy covariance air-sea CO<sub>2</sub> flux measurements and implications for gas transfer velocity parameterisations. *Atmospheric Chemistry and Physics*, 21(10), 8089–8110. <https://doi.org/10.5194/acp-21-8089-2021>
- Edson, J. B., Jampana, V., Weller, R. A., Bigorre, S. P., Plueddemann, A. J., Fairall, C. W., et al. (2013). On the exchange of momentum over the open ocean. *Journal of Physical Oceanography*, 43(8), 1589–1610.
- Else, B. G. T., Galley, R. J., Lansard, B., Barber, D. G., Brown, K., Miller, L. A., et al. (2013). Further observations of a decreasing atmospheric CO<sub>2</sub> uptake capacity in the Canada Basin (Arctic Ocean) due to sea ice loss. *Geophysical Research Letters*, 40(6), 1132–1137. <https://doi.org/10.1002/grl.50268>
- Fairall, C. W., Bradley, E. F., Godfrey, J. S., Wick, G. A., Edson, J. B., & Young, G. S. (1996). Cool-skin and warm-layer effects on sea surface temperature. *Journal of Geophysical Research: Oceans*, 101(C1), 1295–1308. <https://doi.org/10.1029/95JC03190>
- Fischer, T., Kock, A., Arévalo-Martínez, D. L., Dengler, M., Brandt, P., & Bange, H. W. (2019). Gas exchange estimates in the Peruvian upwelling regime biased by multi-day near-surface stratification. *Biogeosciences*, 16(11), 2307–2328. <https://doi.org/10.5194/bg-16-2307-2019>
- Fransson, A., Chierici, M., Miller, L. A., Carnat, G., Shadwick, E., Thomas, H., et al. (2013). Impact of sea-ice processes on the carbonate system and ocean acidification at the ice-water interface of the Amundsen Gulf, Arctic Ocean. *Journal of Geophysical Research: Oceans*, 118(12), 7001–7023. <https://doi.org/10.1002/2013JC009164>
- Fransson, A., Chierici, M., & Nojiri, Y. (2009). New insights into the spatial variability of the surface water carbon dioxide in varying sea ice conditions in the Arctic Ocean. *Continental Shelf Research*, 29(10), 1317–1328. <https://doi.org/10.1016/j.csr.2009.03.008>
- Fransson, A., Chierici, M., Skjelvan, I., Olsen, A., Assmy, P., Peterson, A. K., et al. (2017). Effects of sea-ice and biogeochemical processes and storms on under-ice water fCO<sub>2</sub> during the winter-spring transition in the high Arctic Ocean: Implications for sea-air CO<sub>2</sub> fluxes. *Journal of Geophysical Research: Oceans*, 122(7), 5566–5587. <https://doi.org/10.1002/2016JC012478>
- Jähne, B. (2009). Air-sea gas exchange. In J. H. Steele, K. K. Turekian, & S. A. Thorpe (Eds.), *Encyclopedia ocean Sciences*. Elsevier.
- Landschützer, P., Gruber, N., Bakker, D. C. E., & Schuster, U. (2014). Recent variability of the global ocean carbon sink. *Global Biogeochemical Cycles*, 28(9), 927–949. <https://doi.org/10.1002/2014GB004853>
- Lewis, E. R., & Wallace, D. W. R. (1998). Program developed for CO<sub>2</sub> system calculations. *Environmental System Science Data Infrastructure for a Virtual Ecosystem*. <https://doi.org/10.15485/1464255>
- Li, W. K. W., McLaughlin, F. A., Lovejoy, C., & Carmack, E. C. (2009). Smallest algae thrive as the Arctic Ocean freshens. *Science*, 326(5952), 539. <https://doi.org/10.1126/science.1179798>
- Liss, P. S., & Slater, P. G. (1974). Flux of gases across the air-sea interface. *Nature*, 247(5438), 181–184. <https://doi.org/10.1038/247181a0>
- McPhee, M. G., Proshutinsky, A., Morison, J. H., Steele, M., & Alkire, M. B. (2009). Rapid change in freshwater content of the Arctic Ocean. *Geophysical Research Letters*, 36(10). <https://doi.org/10.1029/2009GL037525>
- Miller, L. A., Burgers, T. M., Burt, W. J., Granskog, M. A., & Papakyriakou, T. N. (2019). Air-sea CO<sub>2</sub> flux estimates in stratified arctic coastal waters: How wrong can we be? *Geophysical Research Letters*, 46(1), 235–243. <https://doi.org/10.1029/2018GL080099>
- Nightingale, P. D., Malin, G., Law, C. S., Watson, A. J., Liss, P. S., Liddicoat, M. I., et al. (2000). In situ evaluation of air-sea gas exchange parameterizations using novel conservative and volatile tracers. *Global Biogeochemical Cycles*, 14(1), 373–387. <https://doi.org/10.1029/1999GB900091>
- Perovich, D., Meier, W., Tschudi, M., Hendricks, S., Petty, A. A., Divine, D., et al. (2020). *Arctic report card 2020: Sea ice*. U. S. N. O. and A. O. of O. and A. R. P. M. E. L. (U.S.), T. S. of Engineering, N. S. and I. D. C. (U.S.), U. of C. (Boulder campus), H. C. for P. and M. R. Alfred-Wegener-Institut für Polar- und Meeresforschung/Alfred Wegener Institute, G. S. F. Center. <https://doi.org/10.25923/n170-9h57>
- Perovich, D. K., Light, B., Eicken, H., Jones, K. F., Runciman, K., & Nghiem, S. V. (2007). Increasing solar heating of the Arctic Ocean and adjacent seas, 1979–2005: Attribution and role in the ice-albedo feedback. *Geophysical Research Letters*, 34(19), L19505. <https://doi.org/10.1029/2007GL031480>
- Prytherch, J., Brooks, I. M., Crill, P. M., Thornton, B. F., Salisbury, D. J., Tjernström, M., et al. (2017). Direct determination of the air-sea CO<sub>2</sub> gas transfer velocity in Arctic sea ice regions. *Geophysical Research Letters*, 44(8), 3770–3778. <https://doi.org/10.1002/2017GL073593>
- Prytherch, J., & Yelland, M. J. (2021). Wind, convection and fetch dependence of gas transfer velocity in an Arctic sea-ice lead determined from eddy covariance CO<sub>2</sub> flux measurements. *Global Biogeochemical Cycles*, 35, e2020GB006633. <https://doi.org/10.1029/2020GB006633>
- Romanovsky, V., Callaghan, T. V., Johansson, M., Bonsal, B., Christiansen, H. H., Instanes, A., & Smith, S. A. (2017). Changing permafrost and its impacts. In *Snow, water, ice and permafrost in the Arctic*. SWIPA. Retrieved from <http://hdl.handle.net/11374/1931>
- Rudels, B., Björk, G., Nilsson, J., Winsor, P., Lake, I., & Nohr, C. (2005). The interaction between waters from the Arctic Ocean and the Nordic Seas north of Fram Strait and along the East Greenland Current: Results from the Arctic Ocean-O<sub>2</sub> Oden expedition. *Journal of Marine Systems*, 55(1–2), 1–30. <https://doi.org/10.1016/j.jmarsys.2004.06.008>
- Rysgaard, S., Glud, R. N., Sejr, M. K., Bendtsen, J., & Christensen, P. B. (2007). Inorganic carbon transport during sea ice growth and decay: A carbon pump in polar seas. *Journal of Geophysical Research: Oceans*, 112(3), 1–8. <https://doi.org/10.1029/2006JC003572>
- Spreen, G., Kaleschke, L., & Heygster, G. (2008). Sea ice remote sensing using AMSR-E 89-GHz channels. *Journal of Geophysical Research: Oceans*, 113(C2). <https://doi.org/10.1029/2005JC003384>
- Takahashi, T., Olafsson, J., Goddard, J. G., Chipman, D. W., & Sutherland, S. C. (1993). Seasonal variation of CO<sub>2</sub> and nutrients in the high-latitude surface oceans: A comparative study. *Global Biogeochemical Cycles*, 7(4), 843–878. <https://doi.org/10.1029/93GB02263>
- Takahashi, T., Sutherland, S. C., Wanninkhof, R., Sweeney, C., Feely, R. A., Chipman, D. W., et al. (2009). Climatological mean and decadal change in surface ocean pCO<sub>2</sub>, and net sea-air CO<sub>2</sub> flux over the global oceans. *Deep Sea Research Part II: Topical Studies in Oceanography*, 56(8–10), 554–577. <https://doi.org/10.1016/j.dsr2.2008.12.009>
- Van Heuven, S., Pierrot, D., Rae, J. W. B., Lewis, E., & Wallace, D. W. R. (2011). *MATLAB program developed for CO<sub>2</sub> system calculations*. ORNL/CDIAC-105b.
- Wanninkhof, R., Asher, W. E., Ho, D. T., Sweeney, C., & McGillis, W. R. (2009). Advances in quantifying air-sea gas exchange and environmental forcing. *Annual Review of Marine Science*, 1(1), 213–244. <https://doi.org/10.1146/annurev.marine.010908.163742>
- Weiss, R. F. (1974). Carbon dioxide in water and seawater: The solubility of a non-ideal gas. *Marine Chemistry*, 2(3), 203–215. [https://doi.org/10.1016/0304-4203\(74\)90015-2](https://doi.org/10.1016/0304-4203(74)90015-2)
- Woolf, D. K., Land, P. E., Shutler, J. D., Goddijn-Murphy, L. M., & Donlon, C. J. (2016). On the calculation of air-sea fluxes of CO<sub>2</sub> in the presence of temperature and salinity gradients. *Journal of Geophysical Research: Oceans*, 121(2), 1229–1248. <https://doi.org/10.1002/2015JC011427>
- Yamamoto-Kawai, M., McLaughlin, F. A., Carmack, E. C., Nishino, S., & Shimada, K. (2009). Aragonite undersaturation in the Arctic Ocean: Effects of ocean acidification and sea ice melt. *Science*, 326(5956), 1098–1100. <https://doi.org/10.1126/science.1174190>

- Yang, M., Bell, T. G., Blomquist, B. W., Fairall, C. W., Brooks, I. M., & Nightingale, P. D. (2016). Air-sea transfer of gas phase controlled compounds. In *IOP Conference Series: Earth and Environmental Science*. IOP Publishing. <https://doi.org/10.1088/1755-1315/35/1/012011>
- Yasunaka, S., Siswanto, E., Olsen, A., Hoppema, M., Watanabe, E., Fransson, A., et al. (2018). Arctic Ocean CO<sub>2</sub> uptake: An improved multiyear estimate of the air-sea CO<sub>2</sub> flux incorporating chlorophyll a concentrations. *Biogeosciences*, *15*(6), 1643–1661. <https://doi.org/10.5194/bg-15-1643-2018>